All-Optical Cascaded Laser Wakefield Accelerator Using Ionization-Induced Injection

J. S. Liu,[1] C. Q. Xia,[1] W. T. Wang,[1] H. Y. Lu,[1] Ch. Wang,[1] A. H. Deng,[1] W. T. Li,[1] H. Zhang,[1] X. Y. Liang,[1] Y. X. Leng,[1] X. M. Lu,[1] C. Wang,[1] J. Z. Wang,[1] K. Nakajima,[1,2] R. X. Li,[1,*] and Z. Z. Xu[1,†]

[1]*State Key Laboratory of High Field Laser Physics, Shanghai Institute of Optics and Fine Mechanics, Chinese Academy of Sciences, Shanghai 201800, China*

[2]*High Energy Accelerator Research Organization, 1-1 Oho, Tsukuba, Ibaraki 305-0801, Japan*

(Received 8 March 2011; published 11 July 2011)

We report on near-GeV electron beam generation from an all-optical cascaded laser wakefield accelerator (LWFA). Electron injection and acceleration are successfully separated and controlled in different LWFA stages by employing two gas cells filled with a He/O_2 mixture and pure He gas, respectively. Electrons with a Maxwellian spectrum, generated from the first LWFA assisted by ionization-induced injection, were seeded into the second LWFA with a 3-mm-thick gas cell and accelerated to be a 0.8-GeV quasimonoenergetic electron beam, corresponding to an acceleration gradient of 187 GV/m. The demonstrated scheme paves the way towards the multi-GeV laser accelerators.

DOI: 10.1103/PhysRevLett.107.035001 PACS numbers: 52.38.Kd, 41.75.Jv, 52.35.Mw

The past few years have witnessed major breakthroughs in the field of electron acceleration based on the laser wakefield accelerator (LWFA) concept [1–4]. Quasimonoenergetic (QM) electron beams (*e* beams) with energies up to 1 GeV have been generated via a centimeter-scale gas-filled capillary discharge waveguide LWFA [5–7]. Self-guided LWFAs in gas jets via self-injection in the "blowout" or "bubble" regime have limited energy gain up to 1 GeV due to the required high plasma density in this approach [8–11]. Experimental results and numerical simulations indicate that a plasma density less than $2 \times 10^{18}\ \mathrm{cm}^{-3}$ is required to produce multi-GeV *e* beams, because a long dephasing length can be obtained and the instability due to relativistic self-focusing can be minimized [12]. However, in this low-density case, electrons are difficult to be self-trapped into the plasma wake for a controllable acceleration. External injection relying on the ionization of the inner-shell electrons is effective for low plasma densities and has recently been demonstrated to generate *e* beams with energies well beyond 1 GeV [13]. The advantage of ionization-induced injection is to decrease the required laser intensity and plasma densities for electron trapping [14,15]. However, due to the continuous ionization-induced injection before the pump depletion of driving laser pulses, the accelerated *e* beams are far from a monoenergetic distribution [13–15]. The present acceleration scheme based on a single staged LWFA does not favor generating QM *e* beams beyond 1 GeV since electron injection and acceleration are not independently controlled. If the trapped electrons assisted by the tunnel ionization in the first stage can be seeded into the lower-density plasma wave in the second stage for further acceleration, electron energies can be easily scaled up to multi-GeV with a narrow energy spread.

Cascaded LWFAs provide a promising route to obtain controllable multi-GeV QM *e* beams. Furthermore, the ability to stage together multi-LWFAs is of vital importance for eventually implementing practical 10-GeV and higher-energy laser accelerators, whereby the electrons are repeatedly accelerated by the laser wakefields in a manner similar to the conventional accelerators. Previous proof-of-principle staged acceleration experiments have been demonstrated by the external injection of *e* beams from a conventional accelerator into a plasma-based wave in the self-modulated regime [16–18]. A very low acceleration gradient of 2.8 GV/m was obtained. Several injection scenarios have been designed for cascaded LWFAs [19]. A staged all-optical LWFA in the self-modulated regime was first demonstrated by using two laser beams, but with the *e*-beam output of continuous spectrum and ~20 MeV maximum energy [20]. Some ideas of a two-stage acceleration approach via density-gradient or tunnel-ionization injection have been proposed [11,15,21,22], but not yet been demonstrated experimentally. Matching between the seed *e* beam and the wakefield excited in the acceleration stage is a critical issue in the cascaded scheme.

Here we report on the first near-GeV QM *e* beams generation from an all-optical cascaded LWFA. By using two segments of gas cells (GCs) filled with a He/O_2 mixture and pure He gas, respectively, we separated the ionization-induced injection in the first LWFA from the acceleration in the second LWFA and successfully realized an all-optical cascaded LWFA. Electrons with a Maxwellian spectrum generated from the first LWFA with relatively high plasma density were successfully seeded into the second low-density LWFA with a 3-mm-thick GC and postaccelerated to be a QM *e* beam with energy of 0.8 GeV, corresponding to an acceleration gradient of 187 GV/m in the second LWFA.

Figure 1 shows the schematic of the experimental setup. Two segments of cylindrical GCs were filled with a He/O_2 mixture and pure He gas flows, respectively. The first GC

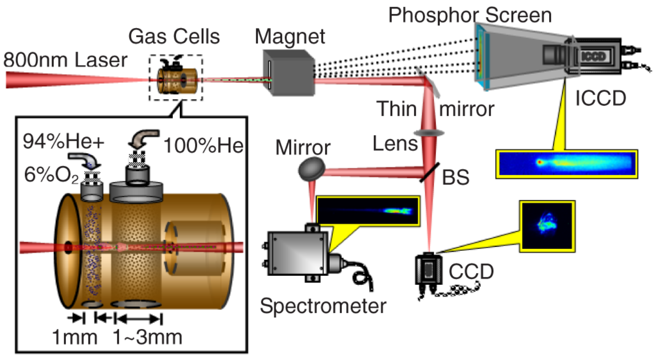

FIG. 1 (color online). Schematic of experimental setup for the cascaded LWFA. BS: beam splitter.

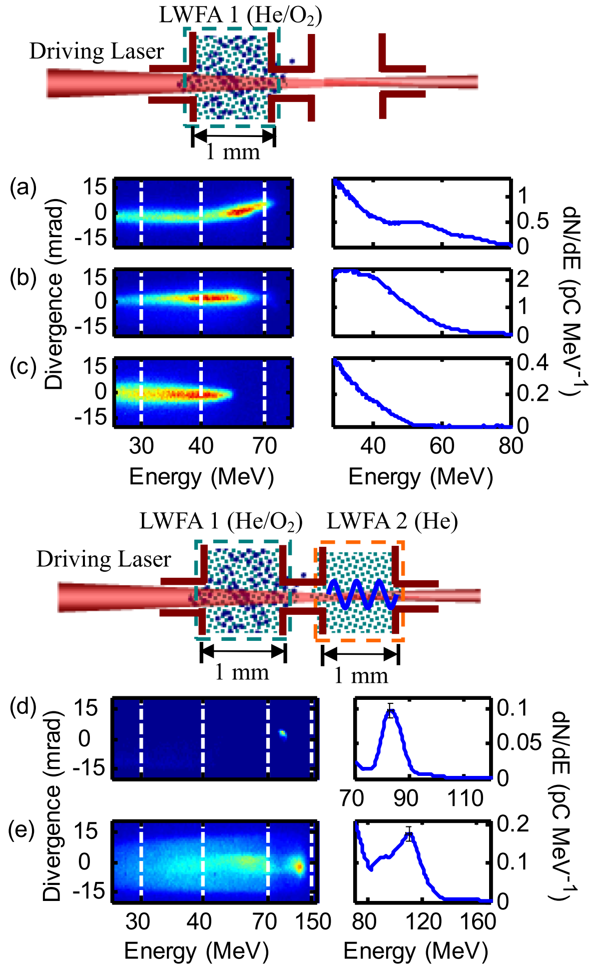

FIG. 2 (color online). (a–c) Single-shot e-beam spectra from the first LWFA. Raw electron spectra (left) and spectra in units of charge per relative energy spread (right) at different focal positions: (a) the focal position $z = 0$, the laser power on the target was 53 TW; (b) $z = 0.6$ mm, 58 TW; (c) $z = 1.2$ mm, 60 TW. (d), (e) Single-shot e-beam spectra from the cascaded LWFA with 1-mm-thick second GC. The laser powers on the target were (d) 48 TW, and (e) 60 TW, respectively.

was 1-mm thick and filled with 6% O_2 gas and 94% He gas flow, the second GC with variable thickness from 1 to 3 mm was filled with pure He gas flow. The amount of oxygen was small (6%) in the first GC in order to reduce the defocusing effect owing to the ionization of the L-shell electrons of oxygen by the leading edge of the laser pulse [15]. In order to avoid mixing the two different gases between these two cells, two pulsed-gas jets with an opening duration of 0.86 ms were used. Each GC was machined with an outlet, which can minimize the counterflow of the forgoing gas flow. The separation between the two cells was 0.5 mm. The hole sizes of the entrance and exit in the GCs for the propagation of the laser beam were 0.5 mm in diameter. The experiments were performed with the femtosecond petawatt laser system [23]. The 40–60 TW laser pulses were used in the experiments. The laser pulses with a duration of 40 fs and central wavelength of 800 nm were focused by an $f/20$ off-axis parabola into the GC. The vacuum beam radius w_0 was measured to be 16 μm at $1/e^2$ of the peak intensity. The fractional laser energy contained within the laser spot was measured to be ~59%. The produced e beams were deflected by a 10-cm-long 0.55-tesla dipole magnet and measured by a Lanex phosphor screen imaged onto an intensified charge-coupled device, which was cross-calibrated by using a calibrated imaging plate to measure the charge of the e beams [24]. The energy resolution of the spectrometer (determined by the e-beam divergence, typically ~3 mrad) was ~10% at 300 MeV and ~25% at 800 MeV. The transmitted light was reflected by a 100-μm-thick glass plate to the forward imaging system for alignment and for transmitted laser spectra measurements by image relaying the exit plane of the plasma column onto the slit of an imaging spectrometer.

Figures 2(a)–2(c) show the measured single-shot e-beam spectra from the first LWFA at different focal positions with laser powers of 50–60 TW (peak intensities of 0.93–1.1 $\times 10^{19}$ W cm^{-2}). The plasma density was $n_e \simeq 5.7 \times 10^{18}$ cm^{-3}, which was measured by using a Michelson-type interferometer [25]. Limited by the exit size of the magnet, only the electrons with energies higher than 27.5 MeV were recorded by the phosphor screen. As the focal spot was moved deeper into the first GC from $z = 0$ (the front wall of the first GC) to $z =$ 1.2 mm, the cutoff energies of e beams with a Maxwellian spectrum decreased from 80 to 50 MeV, and the beam divergence increased from 5 to 8 mrad. The total charges (TCs) of the e beams with energies higher than 27.5 MeV were 25 pC, 56 pC, and 4.6 pC, for Figs. 2(a)–2(c), respectively. When the first GC was filled with pure He gas, no electron was observed if the plasma density was lower than 7.4 $\times 10^{18}$ cm^{-3}. The possibilities of self-injection and density-gradient injection were therefore excluded. Since the input laser intensities used here were lower than the required intensity of 1.8 $\times 10^{19}$ W cm^{-2} for the generation of O^{7+} by tunneling ionization [13], we inferred that ionization-induced injection occurred after the laser intensity increased beyond 1.8 $\times 10^{19}$ W cm^{-2} owing to the self-focusing of the laser beam inside the He/O_2 mixture. As the laser beam was focused at $z = 1.2$ mm, it had to propagate a longer distance to evolve and increase its peak intensity beyond that required intensity, which led to the difference in the TCs and the cutoff energies of the e beams. This assumption was confirmed by the two-dimensional particle-in-cell simulations of the laser pulse evolutions during the propagation in the first GC. The calculations showed that a laser pulse with input power of 45 TW, duration of 40 fs, $w_0 = 15\ \mu$m, and a vacuum focal position at $z = 1.2$ mm was self-focused and guided in the propagation. The laser intensity was increased to $1.8 \times 10^{19}\ \mathrm{W\,cm^{-2}}$ at $z = 0.785$ mm. It was inferred that the K-shell electrons of oxygen were ionized and likely to be injected into the wake in the region $z = (0.8\text{–}1.2)$ mm. At the end of the first-stage plasma, the normalized vector potential was as high as 3. The first LWFA was operated as an electron injector for seeding the second LWFA.

Considering the measured Rayleigh range of the focused laser beam was as short as $\sim$1 mm, we focused the laser beam at the position $z = 1.2$ mm in order to realize the good self-guiding of laser pulses in the second LWFA, as well as the matching between the laser and the plasma wave in the second stage [26]: $k_p w_s = 2\sqrt{a_0}$, where a_0 is the normalized vector potential, and k_p and w_s are plasma wave number and laser spot radius, respectively. Figures 2(d) and 2(e) show the single-shot e-beam spectra from the cascaded LWFA. The thickness of the second GC was 1 mm and the plasma density was $\simeq 2.5 \times 10^{18}\ \mathrm{cm^{-3}}$. As shown in Fig. 2(d) at laser power of 48 TW, a QM e beam peaked at 83 MeV was generated with an energy spread of 9% and a divergence of 2.6 mrad. The TC in this case was 16.2 pC. At laser power of 60 TW as shown in Fig. 2(e), the peak energy of the QM e beam was 110 MeV, which was more than doubled compared to the cutoff energy as shown in Fig. 2(c). The e beam had an energy spread of 27%, a divergence of 7.5 mrad, and a charge of $\sim$5.6 pC, which was higher than the TC obtained in the first LWFA. The TC from the cascaded LWFA was $\sim$87 pC in this case. This result indicated that a great amount of trapped electrons with energies lower than 27.5 MeV in the first LWFA were seeded into the second LWFA for further acceleration. The seed e beams with an almost 100% energy spread were accelerated to be QM e beams by the second LWFA. The maximum acceleration gradient in the second LWFA was estimated to be $\sim$100 GV/m.

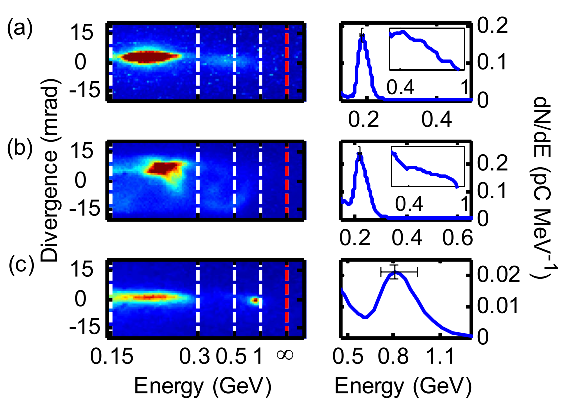

FIG. 3 (color online). Single-shot e-beam spectra from the cascaded LWFA with 3-mm-thick second GC. The laser powers on the target were (a) 50 TW, (b) 48 TW, (c) 45 TW.

The maximum amplitude of the electric field of the plasma wave in the nonlinear regime can be estimated by $E_{\max} = E_0\sqrt{a_0}$ using Lu's model [26] with $E_0 = 96\sqrt{n_e(\mathrm{cm^{-3}})}$. Because of the self-focusing, the laser intensity at the second GC would be as high as $a_0 \approx 3$. The maximum accelerating field was estimated to be $\sim$262 GV/m for $n_e = 2.5 \times 10^{18}\ \mathrm{cm^{-3}}$. The observed accelerating field in the experiment was $\sim 0.38\,E_{\max}$, and thus the location of injected electrons in the plasma wave of the second stage was estimated to be 0.31 λ_p relative to the bubble base, where λ_p is the plasma wavelength. Though the injection phase was not the optimum in the experiments, the successful injection to the plasma wake in the second LWFA was responsible for the observed QM e beams.

Larger energy gains were obtained by increasing the acceleration length in the second LWFA. Figure 3 shows the single-shot e-beam spectra, which were measured when the thickness of the second GC was increased to 3 mm. The plasma densities were $\sim 5.7 \times 10^{18}\ \mathrm{cm^{-3}}$ in the first GC and $\sim 2.5 \times 10^{18}\ \mathrm{cm^{-3}}$ in the second one, respectively. As shown in Figs. 3(a) and 3(b), the QM e beams with peak energy of 185 (216) MeV, 20% (19%) energy spread, 4.4 (6) mrad divergence, and $\sim$10 (23) pC charge were generated by using 50 (48) TW laser pulses, respectively. The maximum energy of the e beams extended up to 0.9 GeV as shown in the insets of Figs. 3(a) and 3(b). However, a QM e beam peaked at 0.8 GeV was observed with 25% energy spread, 2.6 mrad divergence, and $\sim$3.7 pC charge at 45 TW laser power, in addition to the generation of the e beam with continuum spectrum around 200 MeV, as shown in Fig. 3(c). The measured TC was $\sim$320 pC in this case. The energy spread of the generated e beam at 0.8 GeV might actually be less (a few percent) as the energy resolution of our electron spectrometer was limited to 25%. Since the uncertainty in the entrance angle of e beams along the energy dispersion axis was limited to be $\pm$3 mrad by using an input slit, the resulting uncertainty in the peak energy for 0.216 GeV (0.8 GeV) was estimated to be $+4.5\%$, -3.1% ($+19.1\%$, -10.7%). Considering an effective acceleration length of $\sim$4 mm, the highest acceleration gradient of the second LWFA was estimated to be 187 GV/m. It was close to 70% of the above estimated maximum acceleration gradient. In the experiments, almost every laser shot at 50 TW with a power fluctuation of less than 5% resulted in a QM e beam around 200 MeV, but with larger shot-to-shot fluctuations for higher-energy e-beam generation.

The measured transmitted laser spectra as shown in Fig. 4 indicated that the laser pulses were both significantly blueshifted due to the optical field ionization and redshifted by the wake [7,13,15], both of which occurred more intensely when an ultraintense laser pulse was

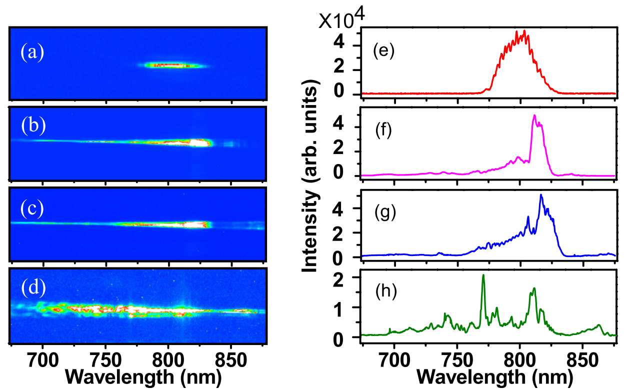

FIG. 4 (color online). Measured transmitted laser spectra at the exit of LWFAs. (a), (e) Original laser spectrum. (b), (f) Typical spectrum after the first LWFA. (c), (g) Typical spectrum after the cascaded LWFA with 1-mm-thick second GC. (d), (h) Typical spectrum after the cascaded LWFA with 3-mm-thick second GC. (a)–(d) Spectrally and spatially resolved spectra. (e)–(h) The corresponding spatially integrated spectra.

self-guided over a longer distance in plasma. The red-shifted light energy which was the spectral intensity integration over the range of 830–875 nm as shown in Fig. 4(g) contained $\sim 3.8\%$ of the total spectral energy when the second GC was 1 mm thick, while it contained $\sim 11\%$ when the second GC was 3 mm thick. These results indicated that in the latter case the laser beam propagated over a longer distance in the second gas flow to excite the plasma wake for acceleration. Furthermore, the measured transmitted laser spectra still contained most of the unshifted light, indicating that the driving laser pulse was far from being depleted, and a thicker GC could be employed for the second LWFA.

In the experiments, no electron with energy higher than 27.5 MeV was observed when the first GC was empty or filled with pure He gas at the same plasma density of $5.7 \times 10^{18}\ \mathrm{cm}^{-3}$. It is reasonable since the plasma density used in the second GC was not high enough for electron self-injection [10,11]. It was confirmed that the observed QM *e* beams were due to the postacceleration in the second LWFA of the *e* beams generated via ionization-induced injection in the first LWFA. Electron injection and efficient acceleration were separately realized.

In order to obtain the maximum acceleration gradient in the second LWFA, electrons should be seeded close to the bubble base of the plasma wave in the second stage. Since the bubble radius of the plasma wave in the second LWFA was larger due to the lower plasma density compared to the first one, lower-energy electrons which were generated in the first LWFA and lagged more behind the laser pulse were favorable for seeding the second LWFA and postacceleration. This might account for the 0.8-GeV *e* beam being generated at a relatively low laser power. Another benefit of focusing the laser pulse close to the second GC was to produce low-energy *e* beams in the first LWFA for the optimization of electron seeding besides the self-guiding in the second LWFA. Properly controlling and optimizing the injection phase of electrons into the second LWFA via manipulating the laser and plasma parameters can ensure the stability of QM *e* beams generation. Here, it is unambiguously demonstrated for the first time that a low-energy *e* beam with a Maxwellian spectrum from an electron injector was captured and then efficiently accelerated by the second low-density plasma column to be a GeV-level QM *e* beam.

In conclusion, we have demonstrated the generation of near-GeV QM *e* beams from an all-optical cascaded LWFA by using tunnel-ionization injection in the first LWFA and optimizing the electron seeding and self-guiding of the laser pulse in the second LWFA. A QM *e* beam with peak energy of 0.8 GeV was obtained by the second LWFA from the seeded *e* beam with a continuum spectrum below 50 MeV, which was generated in the first LWFA. The cascaded LWFA scheme developed here can be scaled up to the generation of multi-GeV *e* beams in a straightforward way by using a long preformed plasma channel as the second LWFA.

This work was supported by the National 973 Program of China (Contract No. 2011CB808100) and NNSF of China (Contracts No. 10974214 and No. 60921004). K. N. was supported by CAS.

*ruxinli@mail.shcnc.ac.cn
†zzxu@mail.shcnc.ac.cn

[1] T. Tajima and J. M. Dawson, Phys. Rev. Lett. **43**, 267 (1979).
[2] S. P. D. Mangles *et al.*, Nature (London) **431**, 535 (2004).
[3] C. G. R. Geddes *et al.*, Nature (London) **431**, 538 (2004).
[4] J. Faure *et al.*, Nature (London) **431**, 541 (2004).
[5] W. P. Leemans *et al.*, Nature Phys. **2**, 696 (2006).
[6] T. P. A. Ibbotson *et al.*, Phys. Rev. ST Accel. Beams **13**, 031301 (2010).
[7] S. Karsch *et al.*, New J. Phys. **9**, 415 (2007).
[8] N. A. M. Hafz *et al.*, Nat. Photon. **2**, 571 (2008).
[9] S. Kneip *et al.*, Phys. Rev. Lett. **103**, 035002 (2009).
[10] D. H. Froula *et al.*, Phys. Rev. Lett. **103**, 215006 (2009).
[11] J. E. Ralph *et al.*, Phys. Plasmas **17**, 056709 (2010).
[12] S. F. Martins *et al.*, Nature Phys. **6**, 311 (2010).
[13] C. E. Clayton *et al.*, Phys. Rev. Lett. **105**, 105003 (2010).
[14] C. McGuffey *et al.*, Phys. Rev. Lett. **104**, 025004 (2010).
[15] A. Pak *et al.*, Phys. Rev. Lett. **104**, 025003 (2010).
[16] F. Amiranoff *et al.*, Phys. Rev. Lett. **81**, 995 (1998).
[17] C. E. Clayton *et al.*, Phys. Rev. Lett. **70**, 37 (1993).
[18] M. Everett *et al.*, Nature (London) **368**, 527 (1994).
[19] V. Malka *et al.*, Phys. Rev. ST Accel. Beams **9**, 091301 (2006).
[20] D. Kaganovich *et al.*, Phys. Plasmas **12**, 100702 (2005).
[21] A. G. Khachatryan *et al.*, Phys. Rev. ST Accel. Beams **10**, 121301 (2007).
[22] R. Trines *et al.*, New J. Phys. **12**, 045027 (2010).
[23] X. Liang *et al.*, Opt. Express **15**, 15335 (2007).
[24] K. A. Tanaka *et al.*, Rev. Sci. Instrum. **76**, 013507 (2005).
[25] Z. Zhou *et al.*, J. Phys. B **43**, 135603 (2010).
[26] W. Lu *et al.*, Phys. Rev. ST Accel. Beams **10**, 061301 (2007).